Influence of Turbulence Modeling On Aftbody Surface Heating Prediction For A Hypersonic Entry Capsule

Kevin Neitzel[1] and Iain D. Boyd[2]
University of Michigan, Ann Arbor, Michigan, 48109, USA

A densely populated aerothermal database based on CFD is needed for the design of a hypersonic entry capsule. Traditionally, this has required the use of low fidelity turbulence models in order to make the computational effort for the large number of CFD runs more tractable. This compromise in accuracy is generally acceptable for the majority of the database. However, comparisons with experimental data have shown that the aftbody heating prediction accuracy is poor for high angle of attack cases. The presence of a large flow separation region appears to be the culprit due to the breakdown of the turbulence modeling assumptions in the region. The presented research investigates the importance of the turbulence modeling in the aftbody heating prediction for high angle of attack cases. The current practice of a simple RANS model is compared with the more sophisticated DES turbulence modeling. The models are investigated for accuracy (compared to experimental data) and for computational cost.

Nomenclature

AOA	=	angle of attack [deg]
B-L	=	Baldwin-Lomax
DES	=	Detached Eddy Simulation
DNS	=	Direct Numerical Simulation
LES	=	Large Eddy Simulation
RANS	=	Reynolds-Averaged Navier Stokes
Re_D	=	Reynolds number based on capsule diameter
SST	=	Shear Stress Transport
T	=	temperature [K]
V	=	velocity [m/s]
ρ	=	density [kg/m^3]

I. Introduction

DEVELOPMENTS in Computational Fluid Dynamics (CFD) as well as dramatic increases in the available computational speed have enabled the use of CFD to develop aerothermal databases for hypersonic vehicle design. (Shuttle was designed using engineering methods - Newtonian theory - with flat/wedge plate and cylinder type assumptions) With larger vehicles, turbulence must be accounted for - typically using Reynolds-Averaged Navier Stokes (RANS) methods. This approach has been proven on a number of science missions[1,2,3] including Mars Science Laboratory (MSL)[4,5] and is considered the current standard practice for much of the aerothermal database calculations. While the computational methods are reliable for attached regions, there remains significant uncertainty in predicting the heating level in the separated wake region, where RANS methods have trouble due to their turbulence modeling assumptions.[6] For ballistic, unguided entries, this can often be overcome with extra design margin. For guided entries with reaction control system (RCS) firing on top of other features in the separated region, the significant margin on the baseline heating level coupled with the various augmentation factors can push the predicted heating level high enough to be greater that many reusable TPS materials can handle.

These separated flow cases necessitate the use of more sophisticated turbulence modeling techniques. Ideally, Direct Numerical Simulation (DNS)[7] would be used to resolve all turbulent flow scales, thus eliminating the modeling assumptions that are present in current methods. DNS on 3-D, real world geometries is all but impossible with today's computational resources and capabilities. For a typical capsule geometry, the grid would have to be

1
American Institute of Aeronautics and Astronautics

resolved to the scale of at least one-millionth the size of the capsule diameter. The most promising turbulence approach is the Detached Eddy Simulation (DES)[8,9] method that uses the RANS method in regions of attached flow and the Large Eddy Simulation (LES)[7] method in regions of separated flow. LES resolves the large turbulent eddy scales that contain the majority of the turbulent kinetic energy and then applies RANS-type models to the smaller turbulent scales. The DES method takes advantage of the computational efficiency of the RANS method where it can accurately model the turbulence (attached flow regions) and applies the more detailed and computationally costly LES method only where it is necessary (separated flow regions).

The presented work focuses on implementing and evaluating turbulence modeling results of the Balwin-Lomax RANS (current standard practice)[10] method and the higher fidelity, DES method that utilizes a the shear stress transport (SST) model for the unresolved scales.[11] A hypersonic entry capsule model has been selected for the presented work because it contains turbulent, separated flow and a large set of experimental data is available for this case. First, the presented paper discusses the case of interest and the associated physics for that condition. The experimental data and numerical approach for the two turbulence modeling methodologies are then outlined. Finally, numerical results for both methodologies are compared with experimental data in order to determine the accuracy and a comment on the relative computational cost is made.

II.   Case of Interest

The case of interest is a high angle of attack and high Reynolds number condition selected from the experimental test matrix for the multi-purpose crew vehicle (MPCV) capsule (conditions shown in Table 1). This case was selected because it represents the prototypical case in which turbulence dominates the flow physics and, for which, the current turbulence modeling appears to be insufficient. The flow conditions and angle of attack produce a large region of separated flow. The Reynolds number leads to primarily turbulent flow in the flow field. This is highly desirable because flow transition is not modeled in this simulation and this situation will reduce any influence that transition may have. Additionally, the flow condition does not exhibit thermochemical nonequilibrium behavior, keeping the turbulence modeling as the dominate variable in the analysis. It should be explicitly stated that the CFD

Case Conditions
$\rho = 0.2402$ kg/m^3
T = 86.6 K
V = 1517 m/s (Mach 8.0)
Re$_D$ = 15x10^6
AOA = 18˚

Table 1. Summary of flow conditions for the case of interest.

Figure 1. Capsule geometry with experimental sting included.

simulations replicate the experimental setup (i.e. the capsule geometry with a portion of the sting balance), as can be seen in Figure 1. Additionally, there are three noteworthy flow features that will be present in the flow field. There is a leading bow shock, prominent shear layer, and large separated flow region. Each of these features needs to be properly captured in order to obtain an accurate representation of the flow physics.

III. Turbulence Physics and Modeling

Turbulence is defined as the flow regime that is characterized by chaotic variations in flow properties. In a classical sense, turbulent flow is made up of different scale eddies. Energy from the bulk flow (large scale) is transferred into the large eddies that tend to become unstable and break up into smaller and smaller eddies. Figure 2 illustrates these vastly differing eddy scales. This process is commonly known as the turbulent energy cascade since kinetic energy is transferred from the larger eddies to the smaller eddies, and it continues until the eddies are sufficiently small that viscosity dominates and the turbulent kinetic energy is dissipated into heat. The scale where this occurs is typically known as the Kolmogorov microscale. For simulation accuracy, one would ideally like to resolve all the eddies scales down to the Kolmogorov microscale (known as Direct Numerical Simulation or DNS). This, however, is not possible for practical problems similar to the one investigated in this study. As the name may suggest, the Kolmogorov microscale is prohibitively small. The ratio of characteristic length scale and the Kolmogorov microscale scales with $Re^{-3/4}$. This means that, for the case of interest, the Kolmogorov microscale is approximately 250,000 times smaller than the diameter of the capsule. The mesh required to resolve all the turbulent scales is not tractable and will not be for quite some time. With this practical limitation in place, it is required that at least some of the turbulent scales must be approximately modeled. The extent to which scales are explicitly resolved and which scales are approximately modeled is the basis of differentiation between several methodologies.
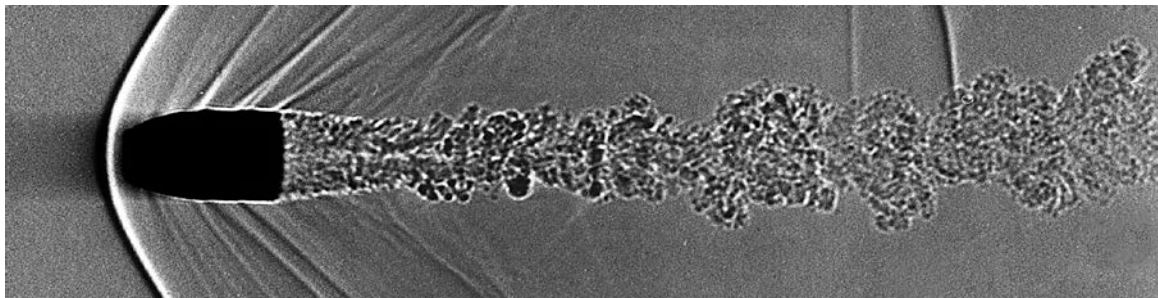

Figure 2. Example flow field that highlights varying turbulent flow scales (Mach 2 bullet – NASA 2007).

The most computationally efficient method investigated in this paper for modeling turbulence is the Reynolds-Averaged Navier Stokes (RANS) method.[8] The method approximately models all turbulence scales by assuming that turbulence is completely random and universal in behavior. There are many forms of RANS turbulence modeling and levels of sophistication. Due to the simplifications made in the modeling approximations, RANS models are only formally applicable to attached flow. The models have been developed over a long period of time and are very accurate for flows that primarily involve attached flow (streamline bodies). Practical experience has shown that RANS can provide agreement with reality for certain cases when there is mild separation, however it is a trial and error process and not based on accurate modeling of the separation physics.

A higher level of fidelity is the method known as Large Eddy Simulation (LES). LES resolves the large eddy scales (mesh size) and models the smaller scales. This method takes advantage of the fact that the majority of the turbulent kinetic energy is contained in the large turbulent eddies. The fact that these turbulent scales must be resolved explicitly dictates that the mesh must be more refined than that of a RANS turbulent method.[2]

Spalart[7] proposed the Detached Eddy Simulation (DES) method in order to resolve the most physics in the most computationally efficient manner. The method combines the RANS method for areas of attached flow (where RANS is known to work well) with the LES method for detached regions of the flow (where additional physics resolution is needed). The method has become very popular, especially for flows with a well-behaved, attached boundary layer for a portion of the body, and separated flow present in another portion. The combination of increased physics capturing and relative computational efficiency make it a promising option for the current investigation. A summary of the various turbulence modeling methods can be found in Figure 3.
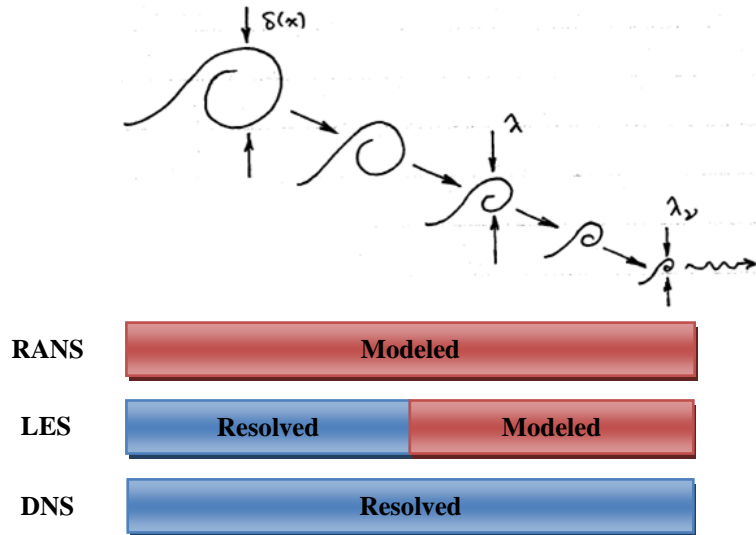
3

American Institute of Aeronautics and Astronautics

Figure 3. Comparison of resolved and modeled turbulent scales for the various turbulence methods.

IV. CUBRC Experimental Data

Experimental runs were conducted in the CUBRC shock tunnel facility.[12] A wide range of flight conditions were studied but the presented work focuses on the flow conditions described in Table 1. The experiments used a scale model (10 cm diameter) of the entry capsule geometry with the aftbody heavily instrumented with thermocouples, as shown in Figure 4. This data represents one of the most complete experimental heat transfer data
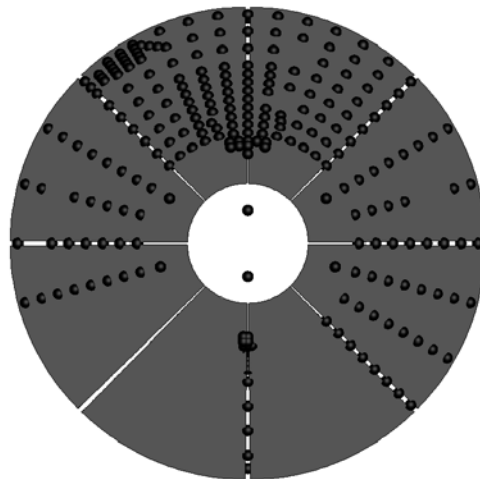
Figure 4. Thermocouple locations for the experimental data (capsule aftbody - rear view).

sets for this geometry to date.

The upper portion of the capsule aftbody is the location of the large separated flow region experienced at the flow condition of interest. The high density of thermocouples makes this data set well suited for comparisons, as well as gaining insight into the adequacy of the numerical models in capturing the underlying physics.

V. Numerical Simulations

All numerical simulations presented are run using the Data Parallel Line-Relaxation (DPLR)[13,14] software from NASA. It is a second-order accurate, upwinding finite-volume method that solves the Navier-Stokes equations. Specifically, it uses a modified form of the Steger-Warming flux-vector splitting scheme and achieves second-order accuracy through a monotone upstream-centered scheme for conservation laws (MUSCL) extrapolation with midmod flux limiter. The code has capability for both block zonal structured grids and overset grids comprised of structured blocks.

A. Current Standard Practice - Block zonal grid with Baldwin-Lomax turbulence model

The grid generation for the standard block zonal grid involves a three step process of initial generation, grid tailoring, and grid mirroring. First, an initial grid is generated utilizing Pointwise. Due to the symmetry of the capsule geometry, the grid is generated from a 2-D definition of the geometry. It is then revolved and grown from the surface to produce a half domain grid. The half domain has the symmetry plane in the pitch plane. The purpose of the half domain at this point is to ensure a symmetric grid in respect to the yaw plane. Also, the domain must be large enough to capture the bow shock in front of the capsule. This can require a trial and error step in the process.

Next, the grid must be tailored to the bow shock in front of the capsule. This procedure increases the accuracy of the simulation in the end by increasing the grid resolution of the shock (improved gradient resolution) and aligning the grid with the shock (improves applicability of the 1-D assumption of flow physics at cell faces). The grid tailoring procedure consists of running the simulation, tailoring the grid, and then iterating those steps until the desired grid quality is achieved. This procedure is completely automated and only requires a select number of parameters to be defined to guide the tailoring. The tailoring acts along the body normal lines of the structured grid. The flow Mach number is the metric used for shock detection. Specifically, the shock location is approximated as the specified fraction of the freestream Mach number (0.95 in this case). Figure 5 illustrates the flow solution on the pitch symmetry plane just prior to the grid tailoring procedure.
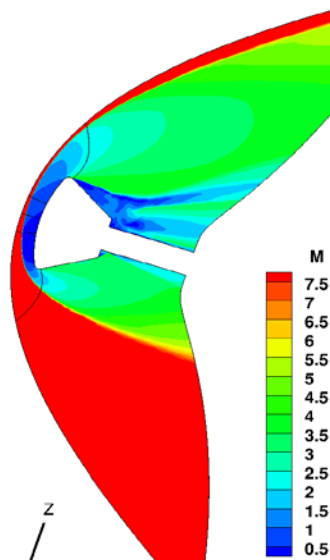

Figure 5. Block zonal mesh from standard practices.

Once the shock location is approximated, the grid points along the body normal direction are redistributed to have a specified portion of pre-shock flow domain, to cluster points near the shock region, and also to enforce a specified cell Reynolds number (as defined below) for the first cell along the capsule surface. The presented work enforced a cell Reynolds number of 1.0 for the surface cells. This ensures consistent and adequately resolved heat transfer calculations.

Finally, the grid must be mirrored in order to produce a fully 3-D grid. Turbulence is a 3-D phenomenon and a symmetric (pitch plane), half model would not adequately capture the physics. The presented grid generation methodology ensures that any 3-D asymmetry in the flow field arises purely from the physics and numerical models, and not from an asymmetric grid. This now represents the final domain used for the simulation. Figure 6 shows the close up of the grid built for this investigation through these standard practices. The grid contains approximately 20 million cells.
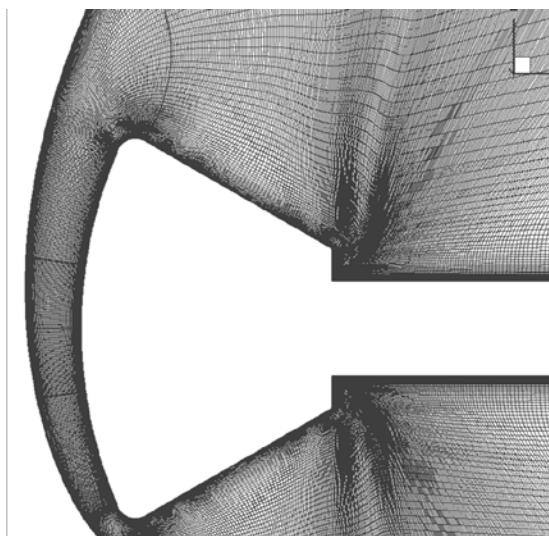

Figure 6. Block zonal mesh from standard practices.

The fact that the grid is block zonal and structured is great for solver performance, however it leads to some undesirable grid characteristics. There is a lack of control over the grid, and thus, grid quality for the regions near the wall. The near wall grid is determined primarily by the surface grid and the bow shock grid tailoring. Qualitatively, the grid on the forebody is very uniform and consistent while the areas around the aftbody have inconsistent size and appear to be much more skewed. This is driven by the more complex shape and turns of the geometry in combination with the structured nature of the grid. For instance, near the rear of the capsule where it merges with the sting geometry, there are spurious "strips" of grid refinement that are attributed to the sharp corners of the geometry.

The flow composition is pure N_2 to replicate the experimental conditions and it is modeled as chemically non-reacting. The simulations do allow for thermal nonequilibrium, however, the results show that there is very little thermal nonequilibrium behavior. The surface thermal boundary condition is a radiative equilibrium condition in which the temperature of the surface is allowed to float such that the radiative heat transfer is in equilibrium with the convective heat transfer. This methodology is the standard practice for flow conditions similar to the case presented.

The surface temperatures and heat flux data presented are time-averaged quantities. The simulation procedure first allows the solution to converge and establish a periodic behavior. Finally, the simulation is run with the surface quantity statistics capability until the time-averaged values settle, and are sample time invariant. This procedure is utilized in order to replicate the processing of the experimental data. Time-resolved data is collected but it is not the focus of the presented work and will not be discussed or compared in this paper.

The algebraic Baldwin-Lomax model is the standard practice turbulence model. This model simply calculates the eddy viscosity from the averaged flow variables. No additional equations are solved and thus it is computationally efficient while still introducing the first level of turbulent physics into the simulation.[15]

B. Higher Fidelity - Overset grid and more sophisticated turbulence model (DES)

An overset grid capability is selected for this investigation because it is able to address a number of the deficiencies observed in the traditional block zonal grids. The two main goals of the overset grid are to improve refinement where it is needed (control) and reduce the skewness in the aftbody region observed in the standard mesh (quality). Both of these goals aim toward the use of DES on this grid. This more sophisticated turbulence modeling technique requires a more refined and higher quality grid since smaller scales are now being explicitly resolved.

In this spirit, four overset grid patches are placed on the standard mesh that is used as the background mesh (see Figure 7). A shear layer grid patch is introduced. This shear layer area is a very important region for turbulent behavior. The high velocity gradient introduces high turbulence production and mesh refinement is needed to explicitly resolve for the small scales in the shear layer. This patch also removes the skewness in the standard mesh within this area. It also better aligns the grid with the flow, which could not be controlled in the standard block zonal grid. Additionally, grid patches are placed near the surface, around the sting, and at the capsule/sting joint. These grid patches aim to remove grid skewness and slightly increase resolution for the DES modeling. The software SUGGAR[16] is used to create the connectivity between patches that is needed in the DPLR flow solver.
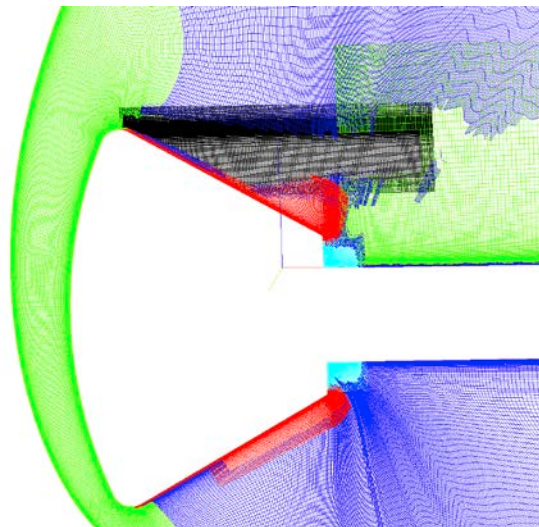

Figure 7. Refined overset grid tailored for DES modeling (Forward Green: forebody , standard mesh; Blue: background, standard mesh; Black: shear layer refinement, Red: surface refinement, Teal: capsule/sting joint refinement; Rear Green: Sting refinement).

The DES method represents the highest fidelity turbulence modeling that is investigated in this work. As previously discussed, DES is more appropriate for flows with large separation since it resolves the highest energy scales of turbulence instead of applying restrictive assumptions to the turbulent behavior as in the Baldwin-Lomax method.[10] The DES method utilizes the RANS turbulence modeling near the wall, in regions of attached flow. Away from the body, the DES implements an LES approach. This approach introduces the local grid size into the model that acts to filter scales so that the scales larger than the grid size are explicitly resolved. The smaller scales are modeled using a subgrid turbulence model such as the SST model in the presented case.

However, this increase in resolving the physics comes at a computational cost. As noted, the grid must be finer to adequately resolve the small turbulent scales. For comparison, the standard grid contains approximately 20

million cells, whereas the high fidelity, overset grid contains approximately 70 million cells. The increase of computational cost of this extra refinement is compounded by the fact that the time step must also be reduced in order to satisfy stability criteria.

VI. Results

The results presented in this paper all correspond to the flow conditions for the case of interest (Table 1).

A. Initial Comparisons - Motivation for the higher fidelity investigation

Figure 8 presents the comparison of time-averaged heat flux between the standard practice numerical simulation and the experimental data. This plot shows that essentially the entire upper half of the aftbody corresponds to a separated flow region. The standard model appears to capture all the general surface features but is not very accurate in the locations of the features. As an example, consider the transition of high heat flux in the bottom section to the lower heat flux area toward the sides and top of the aftbody. The standard model predicts a larger area of high heat flux than the experimental data shows. Perhaps more informative for design purposes and margin development, Figure 9 presents the difference between the results in the form of a percentage, see Equation (1). This plot is quite telling and serves as the main motivation for the higher fidelity modeling investigation. The range of percent difference is selected to be the margin value that is generally placed on these predicted values during design. In this case, the margin on surface heat flux is 50%. It is clear that in the region of large separation, the numerical simulation is underpredicting the heat flux, and the error is beyond the design margin. One other observation is that the percent differences are saturated either high or low for the majority of the data locations. This makes it clear that the models are not accurately capturing the physics of the flow field.

$$\frac{Experiment - Computation}{Experiment} \times 100 \qquad (1)$$
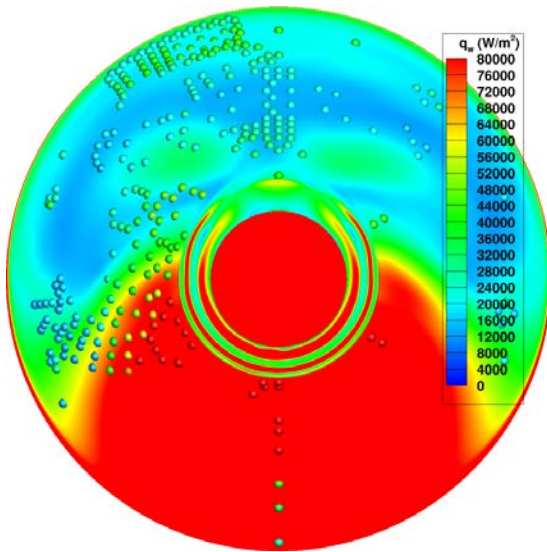

Figure 8. Time-averaged heat flux comparison between the numerical simulation (solid contours) and the experimental data (discrete points).
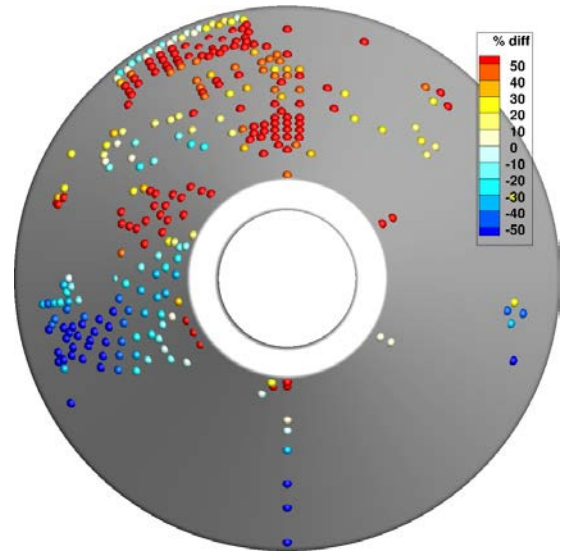

Figure 9. Percent difference between the numerical standard practice solution and the experimental data (Positive percentage: underpredicting; negative percentage: overpredicting).

B. Standard Practice and DES Simulation Comparison

Figures 10 and 11 compare the flow field and surface heat flux at an instant in time (Note that total enthalpy is being plotted for the flow field and heat flux is being plotted on the surface). The higher resolution of the DES/Overset method is apparent in the separated region. Smaller scales in the flow field are being resolved that cannot be seen in the standard practice method. The effect of the high resolution can be seen in the surface quantities as well.
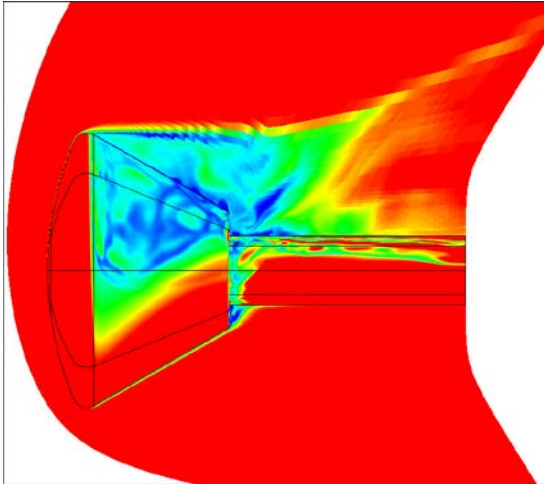

Figure 10. Standard Practice Method Surface and Flow Field Visualization (Flow Field: Total Enthalpy; Surface: Instantaneous Heat Flux)
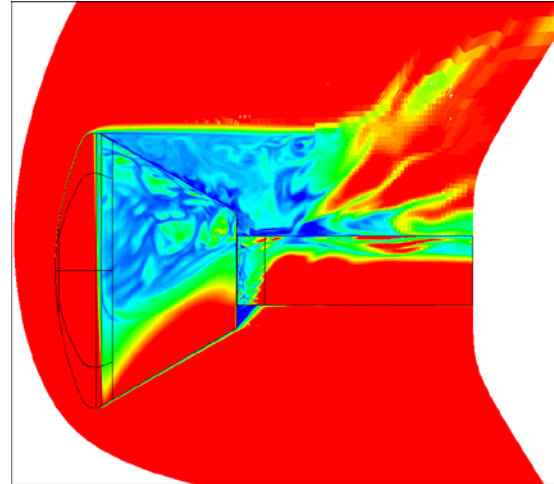

Figure 11. DES/Overset Grid Method Surface and Flow Field Visualization (Flow Field: Total Enthalpy; Surface: Instantaneous Heat Flux)
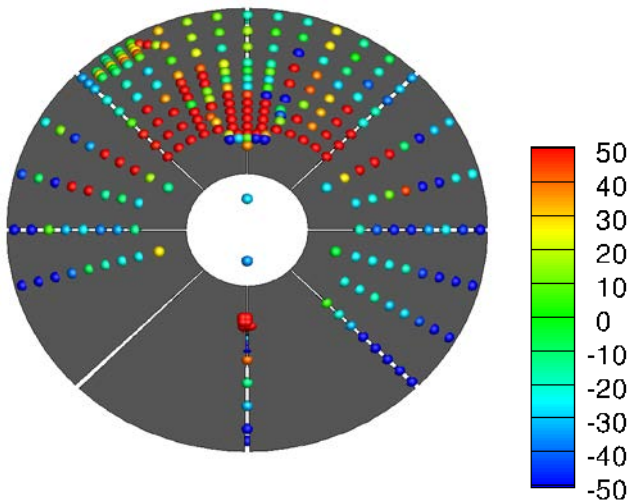

Figure 12. Standard Practice Method: Comparison of Heat Flux with Experimental Data (Percent Difference – Positive: Underpredicting; Negative: Overpredicting)
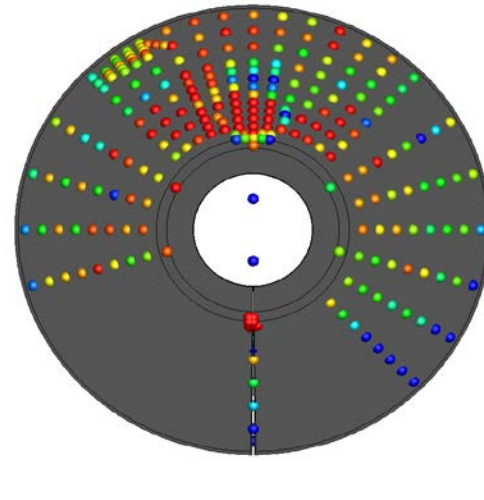

Figure 13. DES/Overset Grid Method: Comparison of Heat Flux with Experimental Data (Percent Difference - Positive: Underpredicting; Negative: Overpredicting)

The standard practice method and DES/Overset method are also compared with the experimental data in Figures 12 and 13. It is qualitatively apparent that the DES/Overset method does provide a more accurate solution (more instances of low error - green). In order to make a quantitative comparison, Table 2 contains the percentage of data locations that lie within the given tolerance. The DES/Overset method shows a quantitative improvement of 13.3% and 7.4% for the ±50% and ±15% tolerance level capturing, respectively. The improvement is expected due to the fact that the high fidelity methodology is accounting for physical phenomena that are most likely important in this flow case.

	±50%	±15%	Below -50%	Above +50%
RANS (B-L)	63.5%	18.1%	13.6%	22.9%
DES/Overset	76.8%	25.5%	6.3%	16.9%

Table 2. Percentage of data point comparisons within the presented tolerances for the two turbulence modeling methods.

Table 2 quantitatively also shows that there is a systemic issue with underprediction (above +50%). Specifically, that underprediction is more prevalent than overprediction, and that improving effect on underprediction for the DES/Overset method is noticeably less than the effect on overprediction. Qualitatively, the majority of the area that is underpredicted is located on the upper, center portion of the aftbody. This area corresponds to the most highly separated region of the flow field and consequently a high turbulent intensity region. Figures 14 and 15 show the ratio of eddy viscosity to molecular viscosity. The figure aims to quantify the extent to which the turbulence is being modeled. RANS analysis only models turbulence so it does not say anything about the resolved turbulence. For DES, however, this provides a metric for grid resolution since it describes the extent to which the turbulence is being resolved on the grid. Ideally for DES, if the grid is resolved enough, the eddy viscosity and molecular viscosity would be on the same order of magnitude (blue). If the eddy viscosity is much larger than the molecular viscosity (red-orange), the turbulent behavior is primarily being modeled (with all of the assumptions and restrictions of the model) and introducing a potentially large source of error in the analysis. Following this logic, it can be seen in the shear layer that the grid is not resolved enough. This helps to explain the underpredicted region. The explanation is plausible since the shear layer region with the high ratio of eddy viscosity to molecular viscosity corresponds very closely with the underpredicted region on the surface. Future studies will work to refine the grid further to confirm this requirement of the analysis implementation.
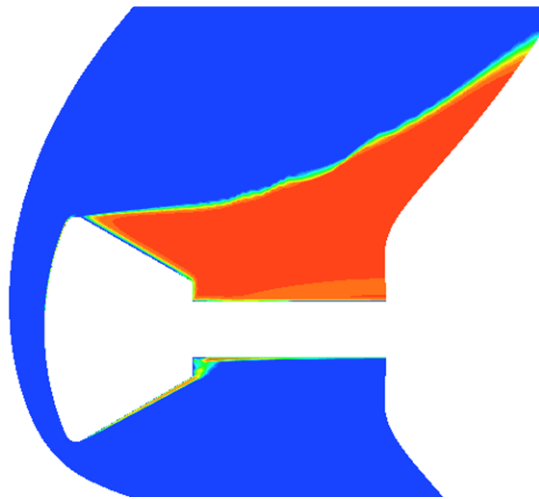
Figure 14.   Standard Practice Method: Ratio of Eddy Viscosity to Molecular Viscosity (Blue:1 – Red:10^4)
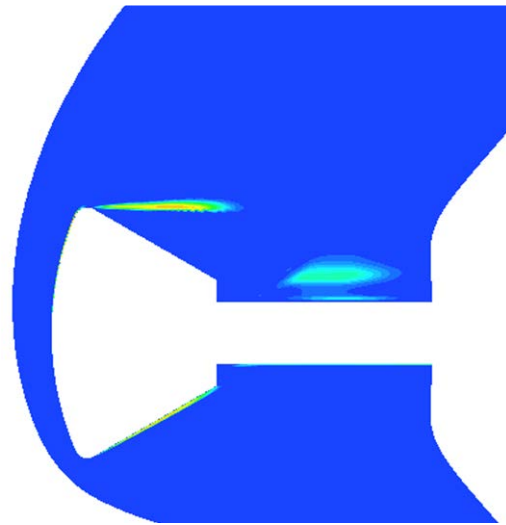
Figure 15.   DES/Overset Grid Method: Ratio of Eddy Viscosity to Molecular Viscosity (Blue:1 – Red:10^4)

One area of concern in all of the simulations is the implementation of the implicit method in the solver. The default solver setting, and the setting used for the presented results, is the line implicit scheme that solves along grid lines normal to the body. This is advantageous for flows with dominant gradients along that body normal direction (i.e. boundary layers and bow shocks). However, in the separated flow region, the gradients are not necessarily in the body normal direction. Utilizing a line implicit scheme in this region may bias the solution along the body normal grid lines. Figure 11 suggests that this may be happening in the region near the shear layer because it is suspiciously sharp and constant in shear layer thickness. One of the follow on investigations will utilize a point implicit scheme in the separated flow grid blocks in an attempt to better capture the physics and eliminate the line bias.

The higher fidelity of the DES/Overset method shows improved results but this is at the expense of computational cost. The standard method has a grid with 20 million cells and requires approximately 6 hours on 200 cores (1,200 CPU hours). The DES/Overset method has a 70 million cell grid and requires approximately 5 days on 800 cores (96,000 CPU hours). Currently, this computational cost is prohibitive in terms of creating the entire design database using the high fidelity, DES/Overset method. The presented methodology of the high fidelity modeling is by no means the most efficient implementation. The presented work aimed to prove the concept and viability for a more accurate analysis. There are many aspects of the implementation that could be improved. The most notable would be the grid resolution. It was shown that more grid resolution should be used in the shear layer but it also appears that much of the increased grid resolution in the overset grid may not be contributing to improved accuracy. A strategic methodology of grid refinement placement could drastically reduce computational cost of the high fidelity modeling.

VII.   Conclusion

A comparison of two turbulence modeling methods was performed for the MPCV hypersonic capsule vehicle using the NASA code DPLR, and the results were evaluated against experimental data. Namely, the influence of the turbulence model on the prediction of surface heat flux was investigated. The standard RANS method using a Baldwin-Lomax turbulence model was implemented on a block zonal grid that was created using standard practices. This methodology has been used successfully for many space missions, but there is significant uncertainty in the results for largely separated flows (due to the breakdown of turbulence model assumptions). The uncertainty is leading to gross underprediction of heating levels in this separated region that is outside the design margin values. A high fidelity, DES method was explored for higher accuracy and to judge the increase in computational cost. The

11

American Institute of Aeronautics and Astronautics

high fidelity model utilized an overset grid to achieve the required resolution for the higher fidelity turbulence model. It also aimed to eliminate cell skewness and cells that are not well aligned with the flow.

The results showed that the DES/Overset method was much better at predicting the surface heat flux levels. The additional turbulence physics that were captured by the high fidelity method are essential to properly predicting the wake flow, and consequently, the surface heat flux. However, the method was very computationally expensive and prohibitive for vast design database work. It should be noted though that the presented implementation was not optimized. The grid resolution in the shear layer proved to be inadequate and some of the grid refinement in other areas proved to be unnecessary in the presented work. In summary, the DES/Overset method is promising in terms of improved surface heating prediction accuracy; however, the computation cost issue must be addressed to make it a viable design methodology.

Acknowledgments

References

[1]Wright, M. J., Prabhu, D. K., and Martinez, E. R., "Analysis of Afterbody Heating Rates on the Apollo Command Modules, Part 1: AS-202," AIAA Paper 2004-2456, June 2004.

[2]Edquist, K.T., Wright, M.J., and Allen, G.A., "Viking Afterbody Heating Computations and Comparisons to Flight Data," AIAA Paper No. 2006-0386, Jan. 2006.

[3]Gupta, R.N., Lee, K.P., and Scott, C.D., "Aerothermal Study of Mars Pathfinder Aeroshell," *Journal of Spacecraft and Rockets*, Vol. 33, No. 1, 1996, pp. 61-69.

[4]Edquist, K., Dyakonov, A., Wright, M., Tang, C., "Aerothermodynamic Environments Definition for the Mars Science Laboratory Entry Capsule," AIAA Paper No. 2007-1206, Jan. 2007.

[5]Edquist, K.T., Dyakonov, A.A., Wright, M.J., and Tang, C.Y., "Aerothermodynamic Design of the Mars Science Laboratory Heatshield," AIAA Paper No. 2009-4075, Jun. 2009.

[6]Strelets, M. (2001), "Detached Eddy Simulation of Massively Separated Flows", AIAA 2001-0879.

[7]Spalart, P. R., Jou, W.-H., Stretlets, M., and Allmaras, S. R. (1997), "Comments on the Feasibility of LES for Wings and on the Hybrid RANS/LES Approach", *Advances in DNS/LES, Proceedings of the First AFOSR International Conference on DNS/LES*.

[8]Brown, J.L., "Turbulence Model Validation for Hypersonic Flows," AIAA Paper No. 2002-3308, Jun. 2002.

[9]Barnhardt, M., Candler, G. (2010), "CFD Analysis of CUBRC Base Flow Experiments", AIAA 2010-1250.

[10]Baldwin, B. and Lomax, H., "Thin Layer Approximation and Algebraic Model for Separated Turbulent Flows," AIAA Paper No. 78-257, Jan. 1978.

[11]Menter, F. R., "Two Equation Eddy-Viscosity Turbulence Models for Engineering Applications," AIAA Journal, Vol. 32, No. 8, 1994, pp. 1598-1605.

[12]MacLean, M., Mundy, E., and Parker, R., "Year 1 Summary Report for Study of Wake Flows on Capsule Bodies," Tech. rep., CUBRC, 2008.

[13]Wright, M., White T., Mangini, N., "Data Parallel Line Relaxation (DPLR) Code User Manual: Acadia Version:4.01.1", NASA TM-2009-215388.

[14]Wright, M. J., Candler, G. V., and Bose, D., "Data-Parallel Line Relaxation Method for the Navier-Stokes Equations," AIAA Journal, Vol. 36, No. 9, 1998, pp. 1603-1609.

[15]Wood, W.A., Kleb, W.L., Hyatt A., (2010), "Assessment of Turbulent CFD Against STS-128 Hypersonic Flight Data", AIAA 2010-4889.

[16]Noack, R. W., "SUGGAR: a General Capability for Moving Body Overset Grid Assembly," 17th AIAA Computational Fluid Dynamics Conference, AIAA Paper 2005-5117, June 2005.